Materials Science & Engineering A 590 (2014) 384–389

Contents lists available at ScienceDirect

Materials Science & Engineering A

journal homepage: www.elsevier.com/locate/msea

Microstructure and mechanical properties of friction spot welds of dissimilar AA5754 Al and AZ31 Mg alloys

U. Suhuddin [a,*], V. Fischer [a,b], F. Kroeff [a,b], J.F. dos Santos [a]

[a] Helmholtz-Zentrum Geesthacht, Centre for Materials and Coastal Research, Institute of Materials Research, Materials Mechanics, Solid State Joining Processes Department, Max-Planck-Str. 1, Geesthacht 21502, Germany
[b] Federal University Rio Grande do Sul, Physical Metallurgy Laboratory, Av. Paulo Gama, 110 Porto Alegre, RS 90040-060, Brazil

ARTICLE INFO

Article history:
Received 2 September 2013
Received in revised form
18 October 2013
Accepted 21 October 2013
Available online 28 October 2013

Keywords:
Friction spot welding
Dissimilar
Intermetallics
Diffusion

ABSTRACT

In the present study, friction spot welding or refill friction stir spot welding was performed to consolidate dissimilar AA5754 Al and AZ31 Mg alloys. The intermetallic compounds of $Al_{12}Mg_{17}$ and Al_3Mg_2 were primarily found in the weld, distributed at the interface between the base materials and in the Al top sheet. The distribution of the intermetallic compounds and the interfacial area between the base materials affect the lap shear strength of the weld. It is concluded that the material flow induced by tool movement plays an important role in both the distribution of the intermetallic compounds and the interfacial area between the base materials.

1. Introduction

To prevent global warming and save energy, industries have put extensive effort into replacing conventional materials with lightweight materials such aluminum (Al) and magnesium (Mg) alloys, e.g., in vehicle structural applications in the transportation sector. Consequently, reliable processes are needed to join such lightweight materials, not only for similar joint configurations but also for dissimilar joint configurations such as Al/Mg alloys, Al/steel alloys, and Mg/steel alloys. Friction-based joining is used in the welding of similar materials [1–5]. However, the process is also an attractive option for welding dissimilar materials [6–12]. Several friction-based joining processes have been used to produce dissimilar joints, including friction stir welding (FSW) [6,8,9] and friction stir spot welding (FSSW) [10,12].

Some studies have shown that the dissimilar welding of Al/Mg alloys using friction-based joining processes [6–12] produces intermetallic compounds (IMCs) of $Al_{12}Mg_{17}$ [6–12], Al_3Mg_2 [6,10], and Mg_2Si [10]. The formation of IMCs is detrimental to the mechanical properties of the joint.

Friction spot welding (FSpW), also known as refill friction stir spot welding, is one of the spot FSW process variants that is used to weld two or more materials in a lap joint configuration. FSpW was developed and patented by GKSS Forschungszentrum Geesthacht (now Helmholtz Zentrum Geesthacht, HZG), Germany. The non-consumable tool used in FSpW consists of three independent moving parts: two rotating sleeve and pin, and a stationary clamping ring. A schematic illustration of the tool and the process is shown in Fig. 1. The stationary clamping ring holds the material against a baking bar in the lap joint configuration, while the rotating sleeve penetrates the materials and the pin moves in the reverse direction. The rotating sleeve introduces plastic deformation and generates frictional heating, which plasticizes the material. The sleeve squeezes the softened material, filling the cavity left by the pin. Then, the rotating sleeve and the pin move back to their initial positions, pushing the softened material back into the joint. Finally, the tool is retracted from the surface, leaving the weld without a keyhole.

As a solid state welding process, FSpW offers many advantages, such as the ability to produce both a weld with good mechanical properties and a weld without a keyhole on the surface [3–5]. FSpW has been successfully used to join similar welds [3–5] and has been used to join dissimilar materials, such as Al and Mg [7]. However, relatively little effort has been made to develop this process, especially in the dissimilar joint configuration. Therefore, the objective of the present study was to investigate the relationship between the grain structure of the spot weld between dissimilar AA5754 Al and AZ31 Mg alloys and its mechanical properties.

2. Experimental procedure

The FSpW process was used to join dissimilar AA5754-H24 Al alloy and AZ31 Mg alloy in the lap joint configuration. The sample

* Corresponding author. Tel.: +49 4152 87 2070; fax: +49 4152 87 2033.
E-mail address: uceu.suhuddin@hzg.de (U. Suhuddin).

0921-5093/$ - see front matter © 2013 Elsevier B.V. All rights reserved.
http://dx.doi.org/10.1016/j.msea.2013.10.057

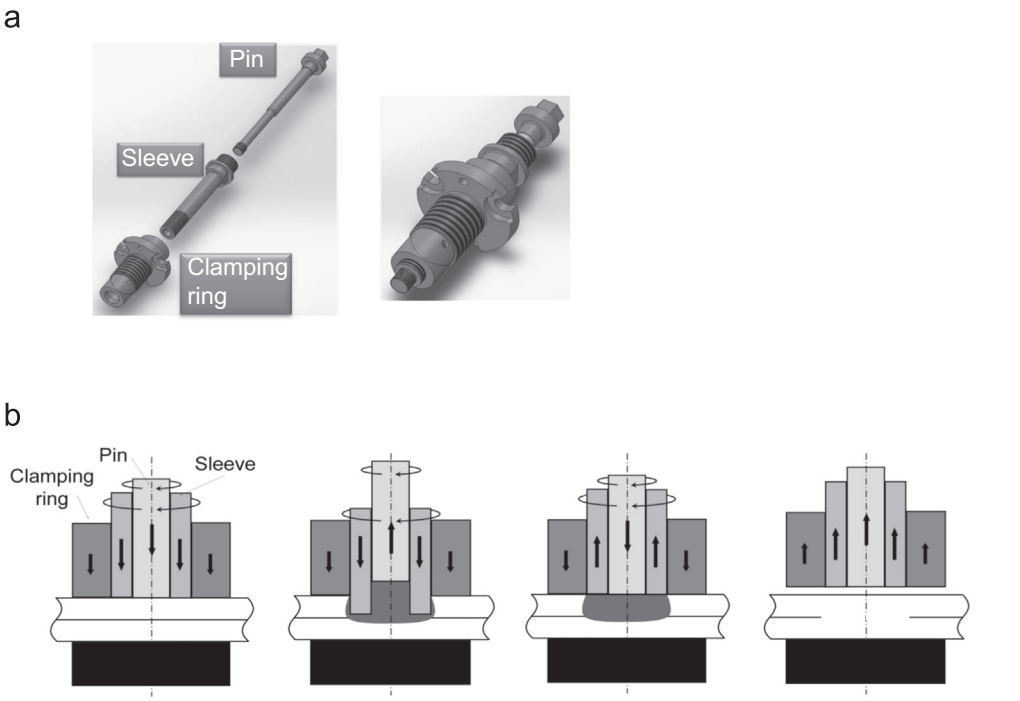

Fig. 1. Schematic illustration of the tool (a) and the friction spot welding process (b).

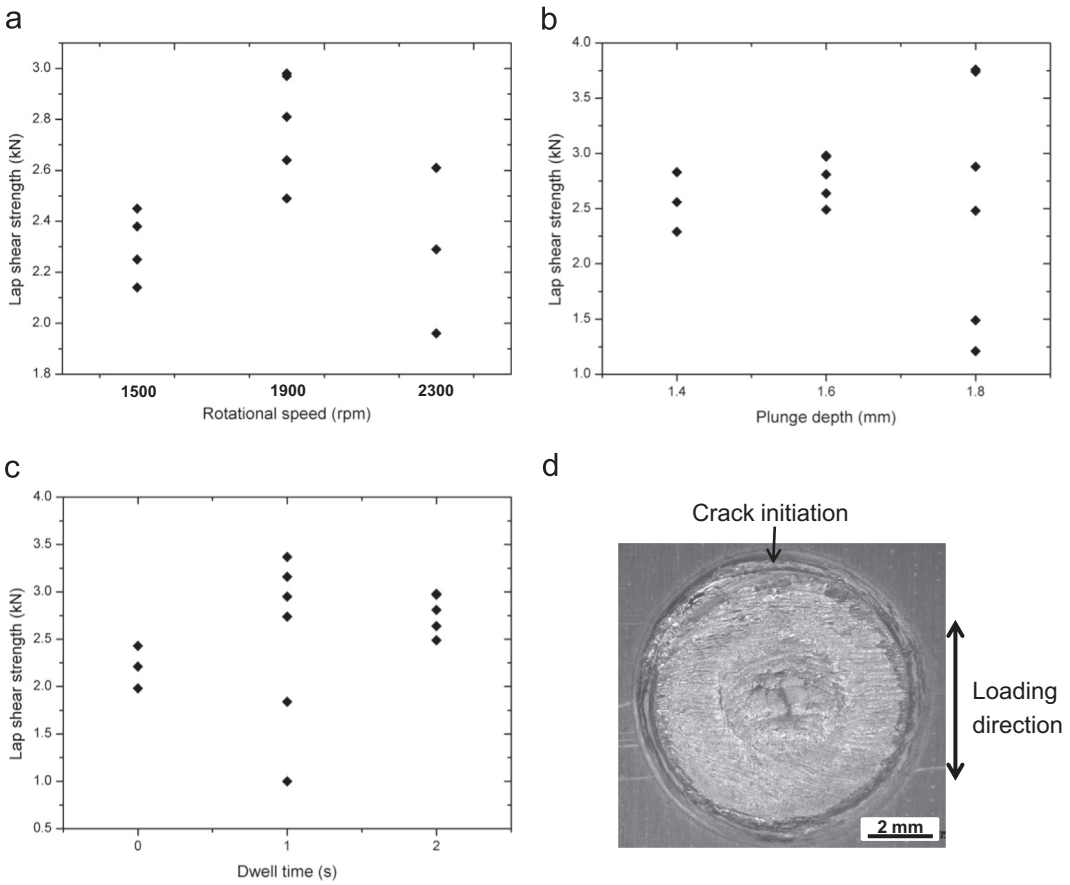

Fig. 2. Effect of the welding parameters on the lap shear strength of the joints (a-c), and an example of the fracture surface (d).

dimension used was $100 \times 25.4 \times 2\ mm^3$ coupons. The process was performed using a RPS 100 machine, using a non-consumable tool with diameters of 14.5 mm, 9 mm and 6 mm for the clamping ring, sleeve and pin, respectively. The sleeve had thread in the outer part to enhance material mixing, as shown in Fig. 1. The Al alloy plate was placed on the Mg alloy plate. The samples were welded using a range of rotational speeds, i.e., 1500–2300 rpm, plunge depths of 1.4–1.8 mm, dwell times of 0–2 s and a clamping

force of 12 kN. The plunging and retracting times were 2 s, regardless of the plunge depth.

To get more insight on the material flow with regard to the IMC distribution during FSpW, additional "stop action" experiments were performed. The welding cycle was stopped by pressing the emergency button during the dwell period. Subsequently, a solution of ice and water was poured onto the sample to freeze the microstructure, hereafter referred to as an "as-quenched sample".

Following the process, the welds were sectioned across the center. Then, they were ground using abrasive paper and polished using colloidal silica, with minimum contact with water. To observe the IMC distribution, the welds were electrolytically etched using a fluoroboric acid-based solution to dissolve the Mg-rich layer or the IMC layer containing Mg.

Microstructure analyses were performed using a Leica DM IRM optical microscope and a FEI Quanta 650 FEG scanning electron microscope (SEM) equipped with an EDAX energy dispersive X-ray spectrometer (EDS). The fracture surface contour was measured using a Keyence VK-9700 laser microscope. X-ray diffraction was used to characterize the fracture surface for phase identification.

3. Results and discussions

3.1. Mechanical properties

The effects of the welding parameters on the lap shear strength (LSS) are presented in Fig. 2. The LSS of the materials have large scatter in the data, with a standard deviation greater than 10%. All samples have the same fracture mode, namely through weld. It is most likely that the crack initiates from the tip of the bonding area and propagates through the brittle IMC commonly formed in the dissimilar Al/Mg weld. An example of the fracture surface is presented in Fig. 2d. Apparently, the relationship between the welding parameters and the LSS is unclear.

To understand more about the factors affecting the LSS, the interfacial areas between the base materials and the IMC distribution were considered. The interfacial areas, which are represented by the length of the fracture surface across the center, were measured using a laser microscope at the top of the Al sheet side. The measurement data are presented in Fig. 3, including an example of the fracture surface as an inset. It is likely that a greater length of the surface contour would increase the LSS.

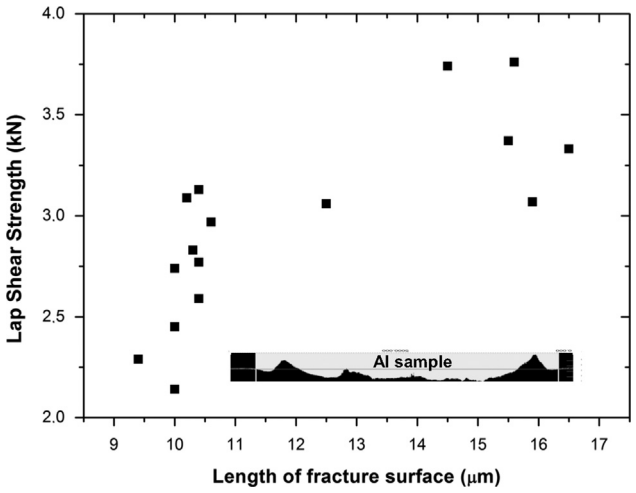

Fig. 3. Effect of the length of the fracture surface on the lap shear strength.

Three welds, with high, medium and low LSSs, were analyzed to clarify the relationship between the microstructure (with regard to the distribution of IMCs) and the mechanical properties. The samples were welded using 1900 rpm rotational speed, 2 s dwell time, 12 kN clamping force, and 2 s plunge and retracting times, with different plunge depths of 1.8 mm, 1.6 mm and 1.4 mm. The welds produced using the depths of 1.8 mm, 1.6 mm and 1.4 mm represent the high, medium and low LSSs, respectively. Fig. 4 presents the macrograph taken from cross-sections of the welds before (Fig. 4a–c) and after etching (Fig. 4d–f). The presence of dark regions in the samples after etching indicates that those regions are Mg-enriched or are IMCs containing Mg.

As can be observed, all of the samples have a relatively large volume of IMCs or Mg-enriched regions; however, the distributions among the samples are different. The dark regions in the high LSS sample are distributed mostly in the vicinity of the Al top surface at the sleeve region, while some of these regions appear in the Al top sheet and at the interfacial area. Conversely, in the medium and low LSS samples, most of the dark regions are situated at the interface in the center region, and some of them are in the Al top sheet. It is likely that the presence of the IMCs at the interface plays an important role in determining the mechanical properties of the joint.

The differences in the distribution of the IMCs material and interfacial area presumably relate to the material flow during welding. To learn about the materials flow, stop action experiments were performed. Fig. 5 presents the macrographs of high, medium and low LSS samples [a–c] as well as micrographs [d–f] taken from the areas marked by rectangles in [a–c] in the as-quenched samples. All samples exhibit cracks across the center of the weld, which were generated during tool removal. Microstructural analyses reveal that all samples exhibit a eutectic phase evidencing the formation of a liquid phase during welding, as presented in Fig. 4d–f. The formation of a eutectic phase during welding is due to the interdiffusion of Al and Mg atoms, and this process is enhanced by the transportation of Mg alloys into the Al top sheet and the formation of fine grain structure during welding [7]. Based on the plunge depth, the weld exhibiting the greater plunge depth should have more Mg alloy material transported into the Al sheet. Thus, high LSS welds should exhibit more liquid phase and/or Mg-rich regions at the interface than the other samples after tool plunging. However, it is likely that most of the liquid phase formed at the interface is swept away from the center during sleeve retraction, as shown in Fig. 4.

As mentioned above, the sleeve and the pin of the tool have diameters of 9 mm and 6 mm, respectively. The volumes of the squeezed materials filling the cavity left by the pin in the samples welded with plunge depths of 1.8 mm, 1.6 mm and 1.4 mm are approximately 64 mm^3, 57 mm^3, and 50 mm^3, respectively. Because the retracting time for all samples was 2 s, the volume flow rates of the material pushed by the pin during the retracting process are approximately 32 $mm^3\,s^{-1}$, 29 $mm^3\,s^{-1}$, and 25 $mm^3\,s^{-1}$ for the high, medium, and low LSS welds, respectively. From these results, it can be concluded that for the higher volume flow rate, the softened material swept more liquid-eutectic phase away than in lower volume flow rate from the weld center toward the Al top sheet. Additionally, the increased material flow rate during sleeve retraction also led to the formation of a greater profile in the Al sheet in the weld center that enlarged the interfacial area between the base materials, as shown in Fig. 4.

However, it should be noted that the LSS of all samples somehow have a large scatter in the data, particularly in the high LSS sample with a 1.8-mm plunge depth. This scatter is most likely due to the presence of a liquid phase during welding. Because of the nature of the liquid phase, the liquid phase might behave differently under deformation, although the welds were welded with the same welding parameters. However, further experimentation is required to clarify this matter.

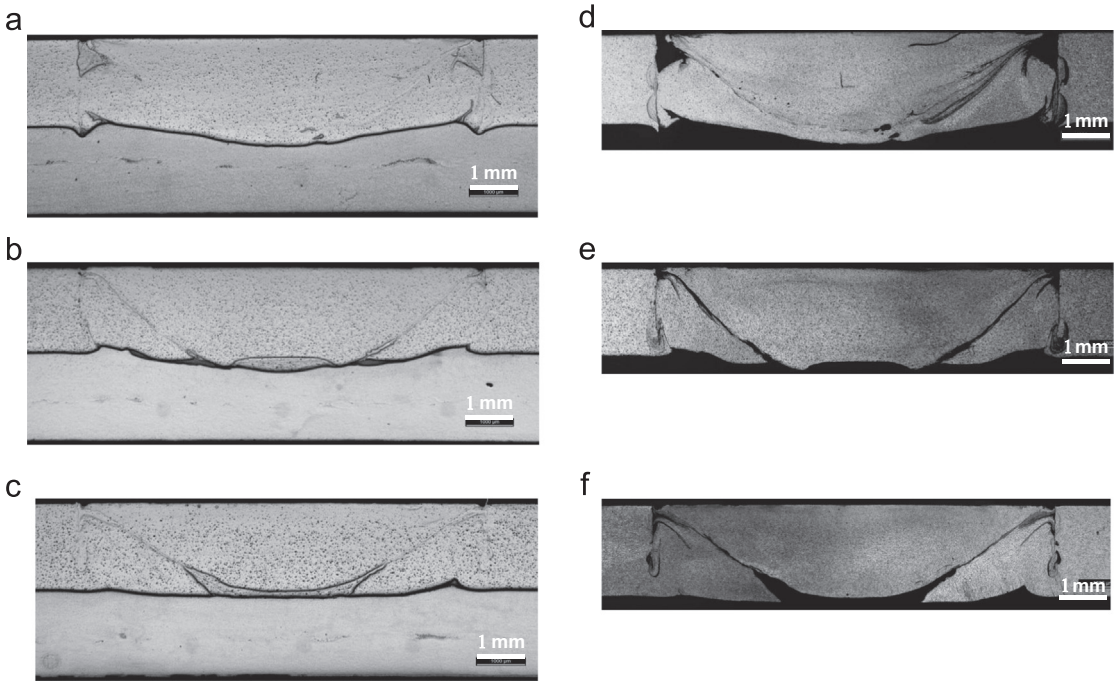

Fig. 4. Micrographs of the sample before (a–c) and after etching (d–f), welded with a difference plunge depth of 1.8 mm (a and d), 1.6 mm (b and e) and 1.4 mm (c and f).

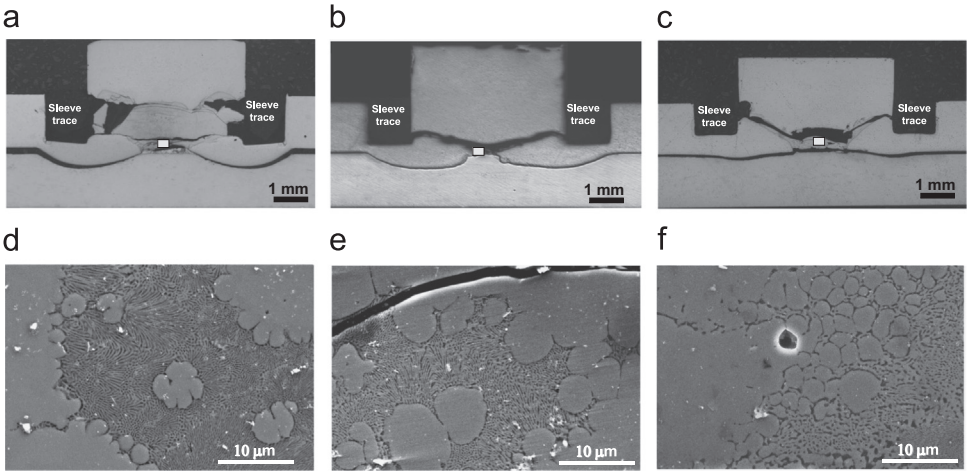

Fig. 5. Low-magnification overview of as-quenched samples (a–c) after stop action experiments produced using plunge depth of 1.8 mm, 1.6 mm and 1.4 mm, and micrographs (d–f) taken from the regions marked with rectangles in (a–c).

3.2. *Microstructure of the joint*

A low magnification overview of the weld with a high LSS is shown in Fig. 6a. The welded area has almost the same thickness as the base material. No keyhole or defect, such as a void or a crack, can be observed. For further understanding, details of some regions are discussed.

An enlarged image taken from region 1 in Fig. 6a is presented in Fig. 6b. The interfacial layer in region 1 has a thickness of approximately 7 μm. EDS analysis across the interfacial layer shows that the composition changes across the interfacial layer in region 1, indicating diffusion during welding, as presented in Fig. 6c. Meanwhile, the interfacial layer in region 2 has a thickness of approximately 20 μm, as shown in Fig. 7a. The layer consists of gray and dark phases that have a Mg composition of approximately 64 at% and 81 at%, respectively. According to the binary equilibrium Al–Mg phase diagram, the gray and dark phases consist of γ-$Al_{12}Mg_{17}$ and δ-Mg in different quantities. A line scan across the layer is presented in Fig. 6b. In addition to the chemical composition gradient, there is an area in which the composition is constant at approximately 64 at% Mg. It is likely that the formation of the interfacial layer in region 2 is not only due to the diffusion process but is also most likely affected by the material flow induced by tool movement during the welding process [7].

Fig. 8a presents an enlarged micrograph taken from region 3 in Fig. 6a, including the chemical composition distribution of Al and Mg, as shown in Fig. 8b and c, respectively. The region is located underneath the sleeve during the welding process. The interface between the materials has an irregular shape. Some Mg elements have been transported into the Al base material, which presumably correspond to the material flow induced by the pin during sleeve retraction. The enlarged microstructure reveals that a eutectic phase

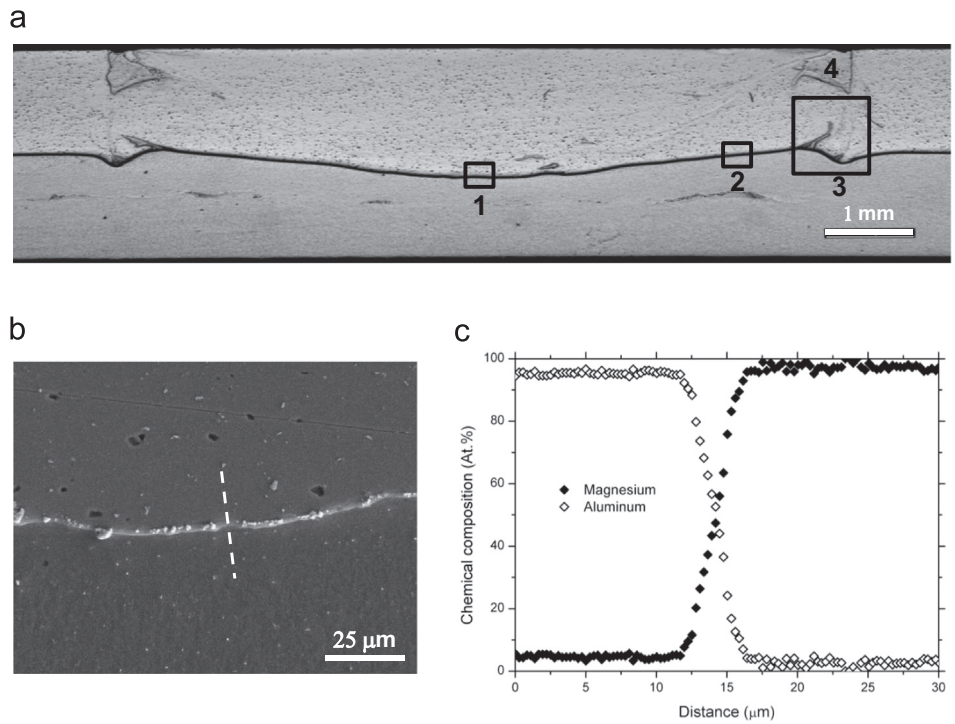

Fig. 6. Macrograph taken from the weld with a high LSS (a), enlarged microstructures from region 1, and its chemical composition distribution (c).

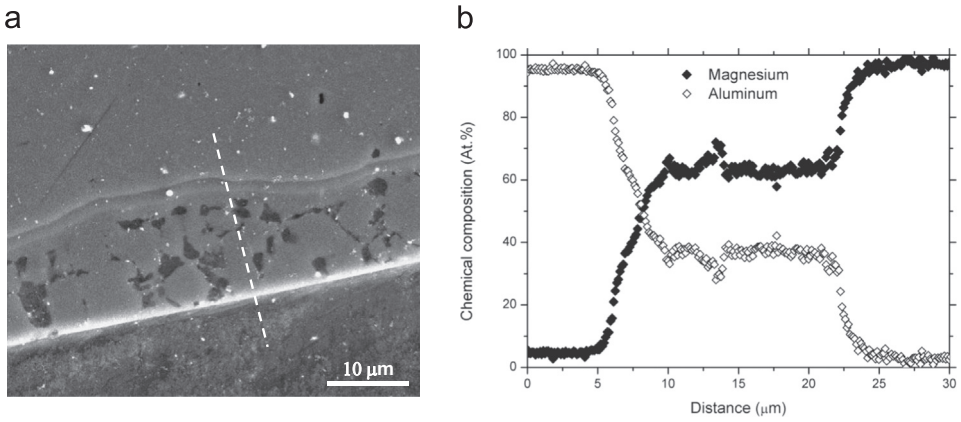

Fig. 7. SEM image taken from region 2 in Fig. 6a (a) and the chemical composition across the interface (b).

has been observed in this region, as shown in Fig. 8d; however, the quantity is less than the amount observed in the as-quenched sample.

Meanwhile, region 4 has only a gray phase exhibiting approximately 35 at% Mg (the micrograph is not shown here). According to the binary equilibrium Al–Mg phase diagram, the region is primarily composed of Al_3Mg_2 and α-Al.

The formation of the $Al_{12}Mg_{17}$ and Al_3Mg_2 in the weld, particularly at the interface, was confirmed by the XRD characterization of fracture surfaces of materials after LSS tests, as shown in Fig. 9.

Microstructure observation reveals that only a small amount of eutectic phase remains in the as-welded samples with a high LSS at the Al and Mg interface, compared with that in the as-quenched samples. Previous study [7] presents that the plastic deformation and high temperature exposure induced by the tool movement during the process lead to the formation of intercalated layers of Al and Mg, and fine grain structure at the interface. The formation of the intercalated layers enlarges the interfacial area between the Al and Mg alloys, while the formation of the fine grain structure means more grain boundaries as diffusion path [13]. Thus, the formation of the intercalated layers [7,9] and fine grain structure [7,13] enhance the interdiffusion of Al and Mg atoms. When the composition of the Al–Mg reached the composition of the eutectic structure, a liquid phase was formed locally. Furthermore, the liquification and solidification occurred repeatedly resulting in formation of large volume of liquid phase which then transformed into eutectic phase, as shown in Fig. 5. A significant reduction of a large volume of eutectic phase in as welded sample most likely relates to the redistribution of the liquid phase and an extensive diffusion process during sleeve retraction [7].

Summary

In the present study, the microstructure and mechanical properties of friction spot welds of dissimilar AA5754-H24 Al alloy and AZ31 Mg alloy have been studied in as-welded and as-quenched samples. The mechanical property that relates to lap shear strength is affected by the area of the fracture surface and

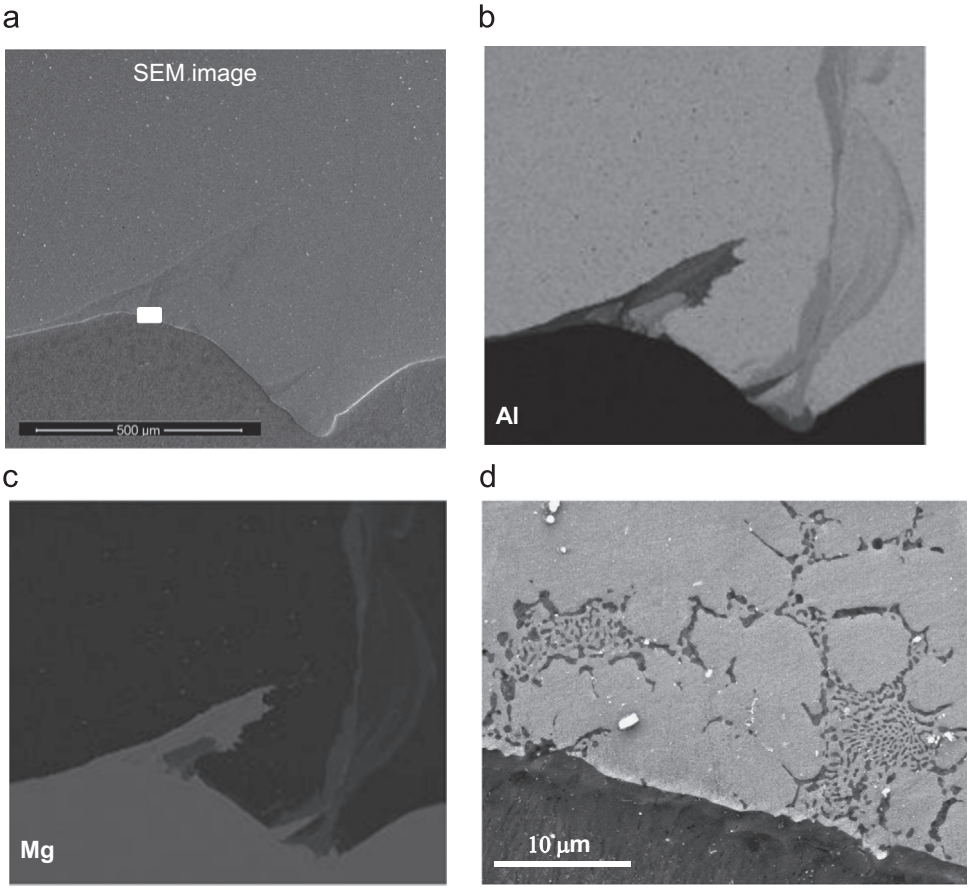

Fig. 8. SEM micrograph taken from region 3 in Fig. 6a (a), the chemical composition mapping of Al (b) and Mg (c), and an enlarged map taken from the region in (a), as indicated by the rectangle (d).

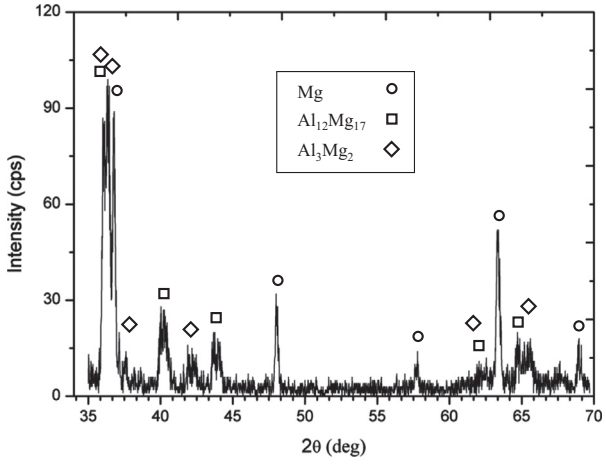

Fig. 9. X-ray diffraction data taken from the fracture surface.

the distribution of IMCs, particularly in the interfacial area. It is likely that the flow of materials induced by tool movement plays important role in the distribution of the IMCs and the interfacial area between the base materials.

The eutectic phase has been observed in the as-quenched sample, indicating the formation of a liquid phase during the process. However, only a small amount of eutectic phase was observed in the as-welded sample due to redistribution of the liquid phase and the extensive diffusion process during sleeve retraction. Chemical analyses by EDS and XRD characterization show that the interfacial area contains $Al_{12}Mg_{17}$ and Al_3Mg_2.

References

[1] L. Commin, M. Dumont, J.-E. Masse, L. Barrallier, Acta Mater. 57 (2009) 326–334.
[2] N. Afrin, D.L. Chen, X. Cao, M. Jahazi, Mater. Sci. Eng. A 472 (2008) 179–186.
[3] T. Rosendo, B. Parra, M.A.D. Tier, A.A.M. da Silva, J.F. dos Santos, T.R. Strohaecker, N.G. Alcantara, Mater. Des. 32 (2011) 1094–1100.
[4] M. Tier, T. Rosendo, C.W. Olea, C. Mazzaferro, F.D. Ramos, M. Beyer, J.F. dos Santos, A.A.M. da Silva, J. Mazzaferro, T.R. Strohaecker, Proceedings of the 7th International Symposium on FSW, Japan, 2008.
[5] L.C. Campanelli, U.F.H. Suhuddin, A.I.S. Antonialli, J.F. dos Santos, N.G. Alcantara, J. Mater. Process. Technol. 213 (2013) 515–521.
[6] A. Kostka, R.S. Coelho, J. dos Santos, A.R. Pyzalla, Scr. Mater. 60 (2009) 953.
[7] U.F.H. Suhuddin, V. Fischer, J.F. dos Santos, Scr. Mater. 68 (2013) 87–90.
[8] R. Zettler, A.A.M. da Silva, S. Rodrigues, A. Blanco, J.F. dos Santos, Adv. Eng. Mater. 8 (2006) 415–421.
[9] Y.S. Sato, S.H.C. Park, M. Michiuchi, H. Kokawa, Scr. Mater. 50 (2004) 1233–1236.
[10] Y.C. Chen, K. Nakata, Scr. Mater. 50 (2008) 433–436.
[11] A. Gerlich, P. Su, T.H. North, Sci. Technol. Weld. Join. 10 (2005) 647–652.
[12] Y.S. Sato, A. Shiota, H. Kokawa, K. Okamoto, Q. Yang, C. Kim, Sci. Technol. Weld. Join. 15 (2010) 319–324.
[13] D.A. Porter, K.E. Easterling, Phase Transformations in Metals and Alloys, Van Nostrand Reinhold, Berkshire, 1981.